ASAR WSS product verification using derived image mosaics

Schubert, Adrian ; Small, David ; Rosich, Betlem ; Meier, Erich

Abstract: A program has been written to create image mosaics from ASA_WSS$_1$ $PASAR-WSSlevel-1products, providinganoverviewoftheimagedarea.Theabilitytogenerate WSSmosaicsfacilitatesthestudyofseveral WSS andfar-rangebackscatterintensities.Radiometriccalibrationisappliedtothemosaics, takingtherange-spreadinglossaswellastheincidenceangleeffectintoaccount, normalisingforsystematicradiometrictrends.Thefive WS 1WSSproducts.$

Originally published at:
Schubert, Adrian; Small, David; Rosich, Betlem; Meier, Erich (2007). ASAR WSS product verification using derived image mosaics. In: Envisat Symposium 2007, Montreux (CH), 23 April 2007 - 27 April 2007. European Space Agency * Communication Production Office, online.

ASAR WSS PRODUCT VERIFICATION USING DERIVED IMAGE MOSAICS

Adrian Schubert[(1)], David Small[(1)], Betlem Rosich[(2)], Erich Meier[(1)]

[(1)] Remote Sensing Laboratories (RSL), University of Zürich, Winterthurerstrasse 190, CH-8057 Zürich, Switzerland, Email: david.small@geo.uzh.ch

[(2)] *ESA-ESRIN, Via Galileo Galilei - 00044 Frascati (ROME), Italy, Email: betlem.rosich@esa.int*

ABSTRACT

A program has been written to create image mosaics from ASA_WSS_1P ASAR-WSS level-1 products, providing an overview of the imaged area. The ability to generate WSS mosaics facilitates the study of several WSS product features. This study focuses on their radiometric and geometric characteristics.

The incidence angle variation of 16 to 43 degrees across beams SS1 through SS5 creates large differences in the nominal near- and far-range backscatter intensities. Radiometric calibration is applied to the mosaics, taking the range-spreading loss as well as the incidence angle effect into account, normalising for systematic radiometric trends.

The five WSS beams acquire data with a substantial overlap (typically several hundred range samples). These overlap regions are of interest because the same ground targets are imaged by two different beams. We calculate the mean radiometric differences between the two beams for each overlap region, and draw conclusions based on the statistics.

WSS geolocation accuracy is assessed for the image mosaics as well, using two methods. First, predicted positions of transponders in the Netherlands and Canada are compared to measured positions. Second, terrain geocoding of selected WSS scenes is performed, using DORIS precise state vectors and a digital terrain model (DTM). The geolocation accuracy is estimated using survey points or ground control points (GCPs) derived from topographic maps.

The radiometric and geometric investigations confirm a high quality of the level-1 WSS products.

1 INTRODUCTION

ASAR Wide-Swath Single-Look Complex (WSS) products differ from conventional focused SAR image products in that the annotated azimuth time is not monotonically increasing, and data from the five subswaths are stored in separate image records.

Generating a WSS mosaic involves resolving separate tasks in the range and azimuth directions. Zero-Doppler azimuth time stamps provide the required information for combining the multiple azimuth "looks" (described in section 2.1), as well as the relative along-track placement of the five subswath image records. In the slant range direction, the subswaths are projected onto a common fast-time (range) grid, with information in the four overlap zones combined in one of three ways (described in section 2). The large mosaic width of ~400 km in the range direction provides a wide dynamic range for two systematic trends, corrected during mosaicking: range-spreading loss and the variation of local illuminated area with nominal incidence angle.

The geometric accuracy of the WSS products are tested by comparing predicted and measured transponder locations in the bursted and mosaicked products.

2 WSS MOSAICKING

An ASAR WSS product is delivered as a single data file containing the subswath data records arranged sequentially. Range and azimuth timing annotations contained within the product specify the extents of the five subswaths, shown in Figure 1 as the blue dotted lines. These extents define the mosaic limits. A typical subswath has a ground-range footprint of ~90 km, and ~9 km (10%) overlap with the adjacent beam(s). Mosaic widths are just over 400 km in range, with an azimuth extent depending on the selected start and stop times.

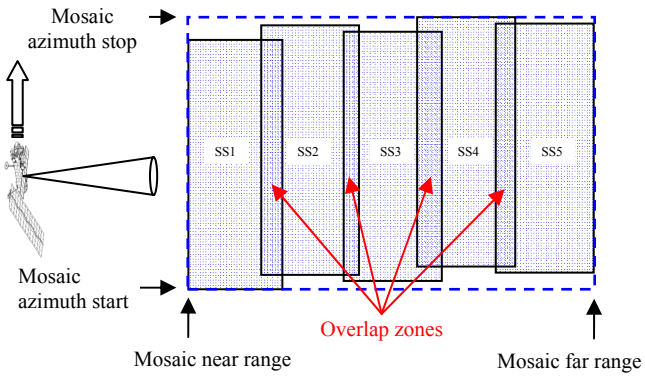

Figure 1. Mosaic extents calculated from input subswath range and azimuth extents

Proc. 'Envisat Symposium 2007', Montreux, Switzerland
23–27 April 2007 (ESA SP-636, July 2007)

2.1 Azimuth Debursting

The ScanSAR technique used to generate WSS products results in a given target being "seen" three times by a given beam, that is, an image is retrieved from three different parts of the azimuth spectrum. These individual "looks" are retained in the level-1 product, and are assigned identical zero-Doppler time stamps. Three such bursts are shown in Figure 2. Azimuth debursting is the process of combining the bursts accordingly, taking the mean of the three "looks" to produce a single "multi-looked" image for each subswath.

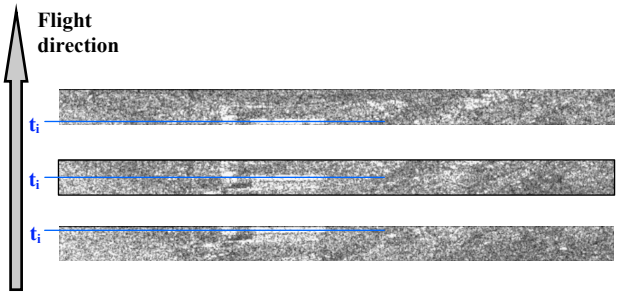

Figure 2. Three bursts containing the same target at zero-Doppler time t_i.

2.2 Range Mosaicking

Azimuth debursting results in five multi-looked one-dimensional arrays: one per subswath. Each array is fast-time-annotated, permitting the transfer of range bins into the output mosaic. Range multilooking can be performed at the same time, with the mean of several input range bins being deposited into a single output bin. The multi-looking factor is calculated initially such that the range and azimuth pixel dimensions are approximately equal at mid-range.

Within the subswath overlap zones (see Figure 1), ground targets are imaged by two beams. It is possible to combine the input samples in one of three ways, the first being the default: (1) the near beam data are used, (2) the far beam data are used, or (3) the mean of the near and far beam data is used. Solution (3) is not preferred because it suppresses the noise slightly in these zones, disturbing the apparent continuity of the mosaic.

3 RADIOMETRY

While the variation due to the elevation AGP has been compensated in the level-1 WSS product, further calibration improves the appearance of the resulting mosaic by "flattening out" two remaining systematic radiometric trends, described in section 3.1.

Section 3.2 describes a method for checking subswath beam calibration relative to the adjacent beam(s). In the beam overlap zones, the same ground targets are imaged from the same look angle by two different beams, making it possible to compare the signals.

3.1 Compensation for Range Effects

WSS level-1 products contain AGP-corrected digital numbers (DN) [1], calculated according to Eq. (1). I and Q are the in- and quadrature phase components of the received complex signal. An example of a mosaic for Resolute, Canada containing the "raw" DNs is shown in Figure 3(a).

$$DN = \sqrt{I^2 + Q^2} \tag{1}$$

$$\beta^0 = \left[\frac{DN_{i,j}^2}{K}\right] \cdot \left[\frac{R_{i,j}}{R_{ref}}\right]^4 \tag{2}$$

$$\sigma^0 = \beta^0 \sin\left(\alpha_{i,j}\right) \tag{3}$$

$$\gamma^0 = \beta^0 \tan\left(\alpha_{i,j}\right) = \frac{\sigma^0}{\cos\left(\alpha_{i,j}\right)} \tag{4}$$

As described in [1], the range-spreading loss is corrected according to Eq. (2) for a pixel at location (i, j). With increasing range $R_{i,j}$ relative to a constant reference R_{ref}, the corrected value given by β^0 is calculated. K is the absolute calibration constant provided in the product annotations, and $\alpha_{i,j}$ is the nominal incidence angle at (i, j). An example of a β^0 image is shown in Figure 3(b).

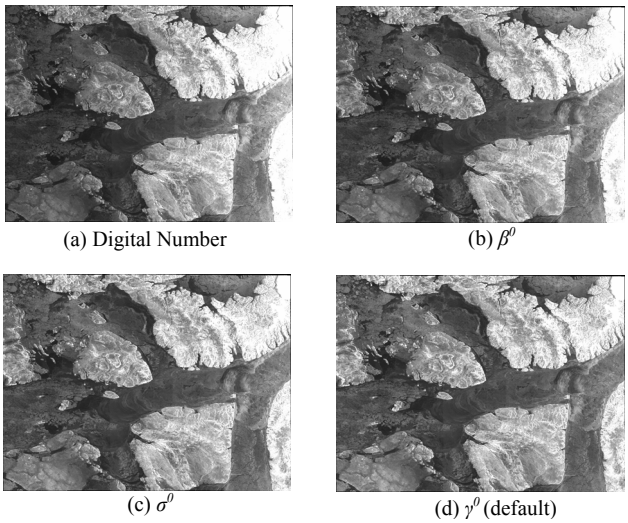

(a) Digital Number (b) β^0

(c) σ^0 (d) γ^0 (default)

Figure 3. Radiometric calibration examples for Resolute, Canada (March 6, 2005; descending orbit 15769)

The variation of the backscatter intensity with changing incidence angle is compensated using one of Eqs. (3) and (4). Multiplying β^0 by the sine of the nominal incidence angle gives σ^0, shown in Figure 3(c). Dividing this result by the cosine of the incidence angle yields γ^0, shown in Figure 3(d). Provision of a γ^0 image

is usually the preferred behaviour, since it is observed to minimise systematic intensity variations between near and far range.

3.2 Beam Differences in Overlap Regions

Figure 4 shows a mosaic produced with four range looks. γ^0 is shown, with near-swath values preferred within range overlap zones. No significant intensity changes are visible between the subswaths. However, the beam overlap regions are of interest because the same ground targets are imaged by two different beams. Within these regions it is therefore possible to choose one beam or the other, or a combination of both. Using mosaics produced exclusively with each possible beam (near and far) and without multi-looking (beyond azimuth debursting), we calculated the radiometric differences for all four overlap zones.

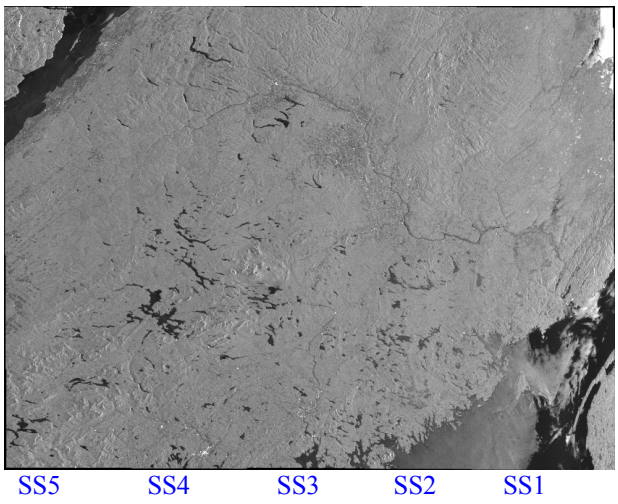

Figure 4. WSS mosaic γ^0, Fredericton, Canada (Oct. 3, 2004, descending orbit 13563)

The following steps were performed:

Two full-resolution mosaics were produced, consisting of uncalibrated digital numbers: one using exclusively near beam values, the other only the far beam.

For each overlap zone (SS1/2, SS2/3, SS3/4, and SS4/5), the ratio of the near-beam to the far-beam data was calculated in two dimensions, generating a "ratio matrix" of the respective image DN values for each overlap zone (DN_{SSnear} / DN_{SSfar}). For locations where at least one beam contained no value, no ratio was calculated.

Each ratio matrix was converted to dB by calculating $10 \cdot \log_{10}(DN_{SSnear} / DN_{SSfar})$.

For each ratio image, the mean value over all azimuth times was calculated for each range bin, generating a one-dimensional array of dB values.

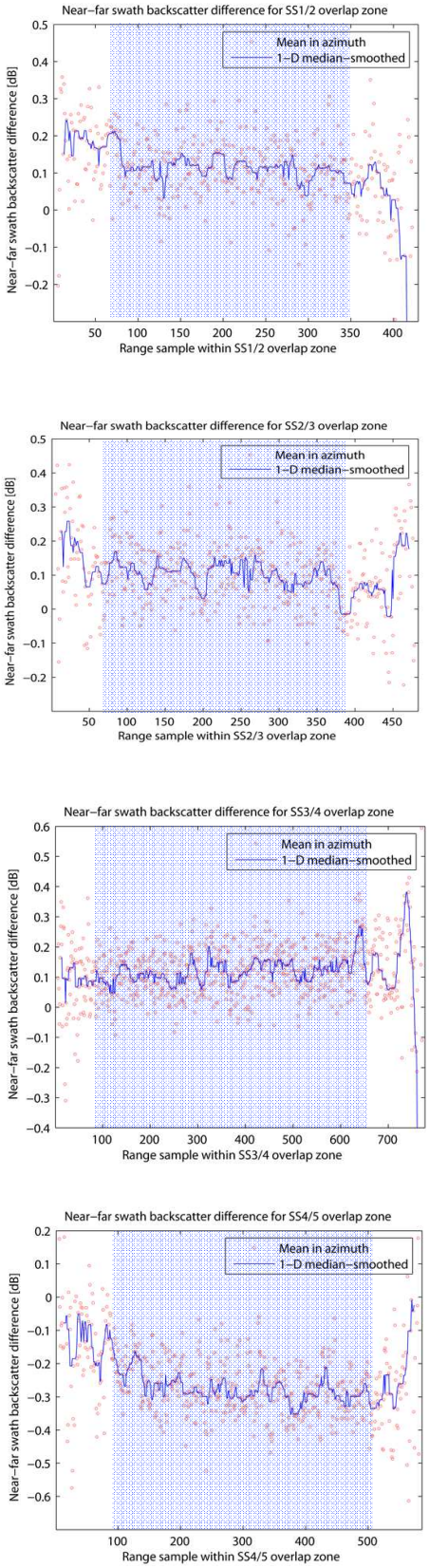

Figure 5. WSS mosaic, Fredericton, Canada (Oct. 3, 2004, descending orbit 13563): Beam overlap differences

Scatter plots were created showing the ratio as a function of range sample in the overlap zone.

A one-dimensional median-smoothing (window size=15) was applied in the range direction for each scatter plot. This was plotted as a solid line on top of the scatter plot to aid interpretation.

The results of these calculations are illustrated in Figure 5. The range extents where the *number* of contributions from each beam are equal are contained within the lightly blue-shaded areas. The data outside of these regions contain a larger number of contributions from one or the other beam, thereby increasing the measurement noise. The most valid beam comparisons are made within the shaded regions indicated.

The first three transitions show mean differences of ~0.10 ± 0.13 dB, with SS4/5 at -0.24 ± 0.13 dB. While these differences are not large, and only slightly disturb the homogeneous appearance of the mosaic, they do indicate small beam calibration differences.

4 GEOMETRIC ACCURACY

The geometric accuracy of WSS products is illustrated below by demonstrating target location prediction, and by terrain geocoding a mosaic.

4.1 Transponder Measurements

Given the radar timing annotations (time of first range sample, range sampling rate, first azimuth time, azimuth sampling rate) and state vectors describing the satellite's trajectory during the time of data acquisition, a point on the Earth's surface may be located within the image by solving the Doppler and range equations in three dimensions [3]. The first range sample time is subject to sampling window start time (SWST) refinement [4]. In some SAR processors, the distance that the satellite moves along-track between sending and receiving a given pulse is not considered in their azimuth timing annotation convention - the small necessary correction can be applied during geolocation [5]. Given the additional consideration of a delay term, the location of radar transponders may be *predicted* within a radar image product and compared to their *measured* positions.

An example of this is given in Figure 6. The γ^0 mosaic is shown in (a). In Figure 6(b) two transponders are imaged (left and right). In each case, the target's predicted location is marked with a blue cross. The zoom level increases towards the bottom. Since a given target is imaged by more than one burst, the additional adjacent bursts that include the same zero-Doppler time annotation are also marked, in yellow.

Figure 6(c) shows the predicted transponder locations in the full-resolution mosaic. No large systematic shifts are visible.

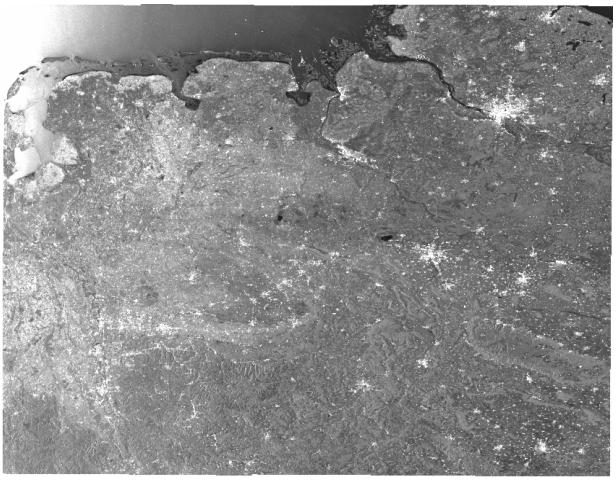

(a) Netherlands & NW Germany WSS mosaic γ^0 (ascending orbit 9330)

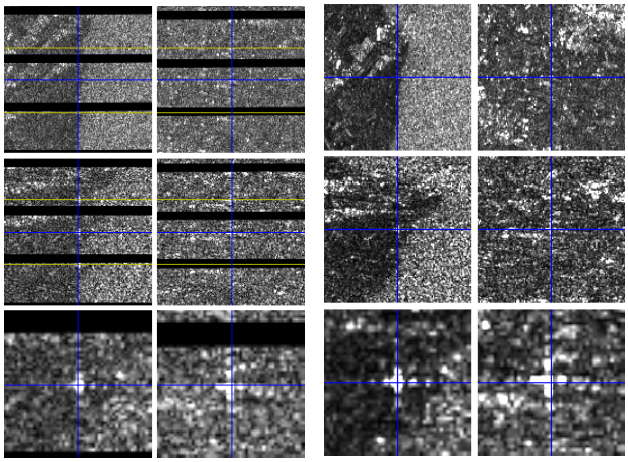

(b) Edam transponder: location predictions in *bursted* product

(c) Zwolle transponder: location predictions in *mosaic*

Figure 6. Netherlands ASAR transponders seen in the bursted and mosaicked data

WSS products produced from acquisitions over four RADARSAT transponders in Canada were also tested. Typical examples are shown for each case in Figure 7. Predictions are within one sample of the measurement for all acquisitions over Resolute and Prince Albert, but there is a small range bias of 3-4 samples (23-31 m) in the Fredericton and Ottawa cases, respectively. The source of this bias is currently under investigation.

As a further test of orbital state vector quality, transponder location predictions were made for five acquisitions over the Resolute transponder. Four types of state vectors were used for the predictions: (1) *predicted* orbits (from the AUX_FPO file), (2) *restituted* orbits (from the AUX_FRO file), (3) *preliminary* orbits (from the DOR_POR file), and *precise* orbits (from the DOR_VOR file). The differences in metres between the predicted and measured locations are listed in Table 1.

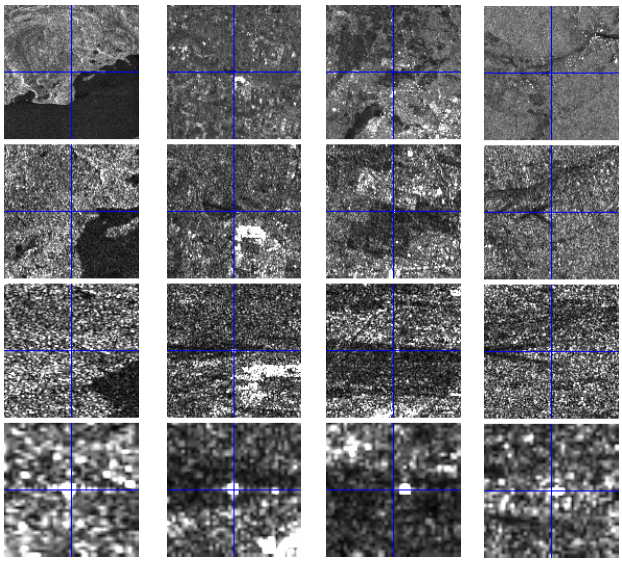

(a) Resolute (b) Prince Albert (c) Ottawa (d) Fredericton

Figure 7. Predicted versus measured RADARSAT transponder locations in Canadian WSS mosaics

Orbit	Predicted AUX_FPO		Restituted AUX_FRO		Preliminary DOR_POR		Precise DOR_VOR	
	Δaz [m]	Δrg [m]	Δaz [m]	Δrg [m]	Δaz [m]	Δrg [m]	Δaz [m]	Δrg [m]
12763	4.4	-1.4	21.5	2.6	23.2	1.8	23.2	1.8
13264	-18.7	-1.6	4.4	2.1	5.6	1.4	5.6	1.4
13765	30.4	-2.4	56.2	1.6	57.4	1.0	57.4	1.1
15769	-36.5	-3.9	-28.9	-0.1	-26.8	-0.3	-26.8	-0.3
17272	-28.7	-0.1	-8.3	3.0	-6.8	2.4	-6.9	2.4
Mean ± σ	-9.8 ± 27.2	-1.9 ± 1.4	9.0 ± 32.2	1.8 ± 1.2	10.5 ± 31.9	1.3 ± 1.0	10.5 ± 31.9	1.3 ± 1.0

Table 1. Summary of location prediction accuracy for the Resolute transponder for different orbit types

The mean and standard deviation values for all acquisitions are summarised at the bottom of the table. All four state vector quality types provide acceptable results for these data sets. The range estimates are especially accurate. The wider distribution in azimuth in all cases is partially due to the relatively low azimuth sample spacing (80 m) in the WSS products & mosaics.

4.2 Terrain Geocoding

As a further test of geometric consistency, a mosaic was created from a WSS product covering the area of Switzerland. The mosaic was terrain-geocoded using a second-generation SRTM 3" digital surface model (DSM). Figure 8 shows the WSS mosaic in its native slant-range geometry.

After terrain geocoding, the mosaic was overlaid with the height model, shown in Figure 9. The SAR image determines the image intensity, while the SRTM height model is presented as an underlying colour cycle with a

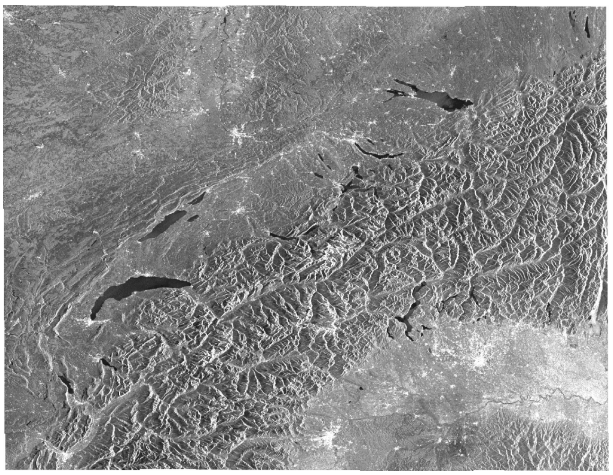

Figure 8. Switzerland: WSS mosaic γ^0

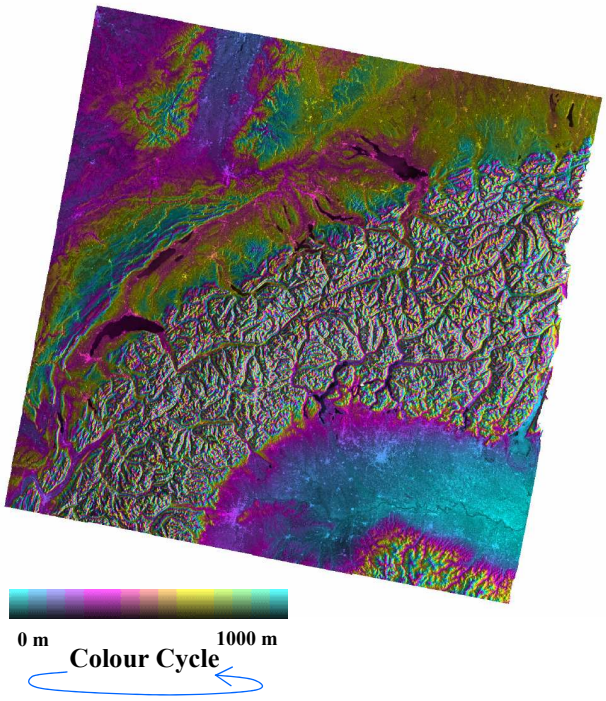

Figure 9. Switzerland: WSS mosaic, terrain geocoded using SRTM 3" (2nd generation)

length of 1000 m. No systematic biases or mislocations are evident.

5 CONCLUSIONS

The radiometric and geometric properties of ASAR WSS products have been investigated by the means of azimuth-debursted, range subswath-concatenated image mosaics.

The resulting ~400 km range width necessitates an adjustment to the WSS digital numbers, correcting for

range spreading loss as well as the variation in local illuminated area with nominal incidence angle.

Small calibration differences of ~0.1-0.2 dB between adjacent beams were detected by inspection of the subswath overlap zones, where the same ground targets are imaged by two different beams.

The localisation accuracy of WSS products was measured using transponder measurements for scenes acquired over the Netherlands and Canada. The range accuracy was seen to be typically within one WSS sample (7.8 m), with occasional biases of up to ~30 m. In azimuth, transponder location predictions were consistently within one WSS sample (80 m).

Additionally, it was seen that all orbital state vector qualities tested yielded WSS mosaics with satisfactory geometric accuracies (within a mosaic sample).

Finally, terrain-geocoding a mosaic over Switzerland using SRTM 3" height data revealed no systematic biases or mislocations in the WSS product.

Our investigations with the image mosaics confirm the high radiometric and geometric quality of ASAR WSS products.

6 REFERENCES

1. Rosich B., Meadows P., Absolute Calibration of ASAR Level 1 Products Generated with PF-ASAR, *ENVI-CLVL-EOPG-TN-03-0010*, Issue 1, Revision 5, ESA-ESRIN, Frascati, Italy, 7 October 2004.
2. Small D., Rosich B., Rosich B., Schubert A., Meier E., ENVISAT ASAR Geometric Validation, *Proc. of CEOS SAR Workshop 2006*, Edinburgh, United Kingdom, Oct. 3-6, 2006 (in press).
3. Small D., Schubert A., Krüettli U., Meier E., Nüesch D., Preliminary Validation of ASAR Geometric Accuracy, *Proc. of ENVISAT Validation Workshop*, Frascati, Italy, Dec. 9-13, 2002 (ESA SP-531, August 2003).
4. Small D., Rosich B., Meier E., Nüesch D., Geometric Calibration and Validation of ASAR Imagery, *Proc. of CEOS SAR Workshop 2004*, Ulm, Germany, May 27-28, 2004.
5. Small D., Rosich B., Schubert A., Meier E., Nüesch D., Geometric Validation of Low- and High-Resolution ASAR Imagery, *Proc. of 2004 ENVISAT & ERS Symposium*, Salzburg, Austria, Sept. 6-10, 2004 (ESA SP-572, April 2005).